


RESEARCH ARTICLE

Open Access



# NLRP3 promotes tumor growth and metastasis in human oral squamous cell carcinoma

Han Wang<sup>1†</sup>, Qingqiong Luo<sup>1†</sup>, Xiaodong Feng<sup>1</sup>, Ruiyang Zhang<sup>1</sup>, Jiang Li<sup>2</sup> and Fuxiang Chen<sup>1\*</sup> 

## Abstract

**Background:** Inflammasomes are reported to be abnormally expressed and activated in several malignancies and play important roles in tumor development. The present study was designed to investigate the expression and function of the NLR family pyrin domain containing protein 3 (NLRP3) inflammasome in oral squamous cell carcinoma (OSCC).

**Methods:** NLRP3 expression in OSCC cell lines and the normal human immortalized oral epithelial cells (HIOEC) was determined by real-time PCR and western blot. Immunohistochemistry was used to examine the expression of NLRP3 and IL-1 $\beta$  in the paraffin-embedded OSCC tissues. The proliferation of OSCC cells was detected by the 3-(4,5-dimethylthiazol-2-yl)-2,5-diphenyl tetrazolium bromide (MTT) assay and cell colony formation ability of the OSCC cells was also evaluated. Tumor cell migration or invasion was measured by the transwell assay and related protein markers were determined by western blot. A mouse xenograft model was established to investigate the OSCC tumor growth in vivo.

**Results:** Significant higher expression of NLRP3 was observed in the OSCC cells. Obvious expression of NLRP3 and IL-1 $\beta$  was found in the paraffin-embedded OSCC tissues, and the NLRP3 expression levels were correlated with the tumor size, lymphnode metastatic status and IL-1 $\beta$  expression. Downregulating NLRP3 expression markedly reduced the cleavage of caspase-1 and production of IL-1 $\beta$  in OSCC cells. NLRP3 knockdown also inhibited the proliferation, migration and invasion of OSCC cells. Further investigation indicated that expressions of E-cadherin and vimentin in OSCC cells were increased, while N-cadherin expression was decreased after NLRP3 knockdown. Downregulating NLRP3 expression in OSCC cells significantly reduced the tumor growth in vivo.

**Conclusions:** Our data suggested that the increased expression of NLRP3 in OSCC was associated with tumor growth and metastasis. NLRP3 may be considered as a potential target for OSCC therapy.

**Keywords:** NLRP3 inflammasome, Oral squamous cell carcinoma, Proliferation, Migration, Invasion

## Background

Oral squamous cell carcinoma (OSCC) is the most common type of cancer in oral cavity, which accounts for more than 90% of all oral cancers [1]. Approximately 300,000 new cases of OSCC patients occurs worldwide annually [2]. Although there are much improvements in multimodality therapy including surgery, radiation and

chemotherapy, the overall survival rate for OSCC still ranges from 50 to 60% [3, 4]. Therefore, it is important to investigate the molecular mechanisms of the occurrence and development of OSCC, which may ultimately help the exploration and establishment of more effective therapeutic strategies.

Chronic inflammation has been reported to play critical roles in carcinogenesis and tumor progression [5–8] and cancer-related inflammation has been recognized as the “seventh hallmark of cancer” [9]. Recently, inflammasomes-mediated inflammation in cancer has aroused great interests in the field [10, 11].

\* Correspondence: [chenfx@sjtu.edu.cn](mailto:chenfx@sjtu.edu.cn)

<sup>†</sup>Equal contributors

<sup>1</sup>Department of Clinical Immunology, Ninth People's Hospital, Shanghai Jiao Tong University School of Medicine, 639 Zhizaoju Road, Shanghai 200011, China

Full list of author information is available at the end of the article



Inflammasomes are large protein complexes typically consisting of the nucleotide-binding and oligomerization domain (NOD)-like receptor (NLR), adapter protein apoptosis-associated speck-like protein containing CARD (ASC) and caspase-1 [12, 13]. Once activated by a diverse range of “danger signals” like oxidative stress, pathogens, metabolic and tissue damage products etc., the inflammasome complex subsequently cleaves pro-IL-1 $\beta$  to its mature bioactive form via the activated caspase-1 [14, 15]. Studies of Fujita et al. reported that the constitutively active NLR pyrin domain-containing protein 3 (NLRP3) inflammasome in human melanoma cells mediated auto-inflammation via caspase-1 processing and IL-1 $\beta$  secretion [16] and NLRP1 inflammasome activation promoted tumor growth in metastatic melanoma [17]. Normand et al. demonstrated the NLRP6 inflammasome controlled epithelial self-renewal and colorectal carcinogenesis upon injury [18]. Kolb et al. indicated obesity associated NLR family CARD domain-containing protein 4 (NLRP4) inflammasome activation drove breast cancer progression [19]. Other investigations have involved inflammasomes in bladder cancer [20], gastric cancer [21], and leukemia [22]. However, the roles of inflammasomes, particularly NLRP3 inflammasome in OSCC have not been fully elucidated.

Thus we performed the present study and found that NLRP3 was aberrantly overexpressed in OSCC cells and tissues. The NLRP3 expression in OSCC tissues was positively correlated with tumor size, lymphonode metastasis status and IL-1 $\beta$  expression (product of the activated NLRP3 inflammsome). Moreover, knockdown of NLRP3 inhibited OSCC cell proliferation, migration and invasion. In the xenograft mouse model, we further demonstrated that suppressing NLRP3 expression could reduce the growth of OSCC in vivo.

## Methods

### Patients and tissue specimens

Seventy-seven primary OSCC tumor samples were collected from patients of Shanghai Ninth People’s Hospital at the Department of Oral and Maxillofacial–Head and Neck Oncology from January 2010 to July 2011, and all the patients had no previous chemotherapy or radiotherapy. The pathological grades were evaluated according to the standard of American Joint Committee on Cancer (AJCC) and all study protocols were approved by the Ethics Committee of the hospital. The clinical parameters of the OSCC patients were included in Table 1.

### Animals

Male BALB/c nude mice about four-week-old were purchased from Shanghai Laboratory Animal Center (Shanghai, China) and kept in animal care facilities under pathogen-free conditions. The procedures of

animal experiments were conducted in line with the institutional guidelines for the use of laboratory animals (The Ministry of Science and Technology of China, 2006) and also had approval of the Ethics Committee of the hospital.

### Cell lines

The human immortalized oral epithelial cells (HIOEC) and three OSCC cell lines- WSU-HN4, WSU-HN6 and CAL27 were kindly provided by the Key Laboratory of Stomatology, Shanghai Ninth People’s Hospital. The OSCC cells were cultured in Dulbecco’s modified Eagle medium (DMEM) (Invitrogen, Carlsbad, CA, USA) supplemented with 1% penicillin-streptomycin and 10% fetal bovine serum (FBS) (Gibco, New York, NY, USA). HIOEC cells were cultured in defined Keratinocyte-SFM (Gibco). All cells were incubated in a humidified atmosphere containing 5% CO<sub>2</sub> at 37 °C.

### Immunohistochemistry (IHC) staining

For IHC staining, the procedures were as described previously [23]. After deparaffinating and rehydrating, the 5  $\mu$ m thick tumor tissue sections were heated by water bath with citric acid buffer for 20 min and blocked in 5% normal goat serum for 30 min, and then incubated with either anti-NLRP3 antibody (1:400, sigma, St Louis, MO, USA) or anti-IL-1 $\beta$  antibody (1:200, Abcam, Cambridge, UK) at 4 °C overnight. Subsequently, the GTVision Two-step Visualization System (Genetech, Shanghai, China) was used to visualize the immunostaining and hematoxylin was used to counter-stain. Finally, the sections were examined under light microscopy and evaluated by the Immuno-Reactive-Score (IRS), which was calculated by multiplying staining proportion score (PS) and staining intensity score (IS). PS was defined as 0 (0%), 1 (1%~25%), 2 (26%~50%), 3 (51%~75%), and 4 (76%~100%). IS was classified as 0 (negative), 1 (weak), 2 (moderate) and 3 (strong). According to the obtained IRS scores, patients were divided into three groups: negative expression group with IRS = 0, weak expression group with IRS = 1~3 and strong positive expression group with IRS = 4~12.

### RNA extraction and real-time PCR

To determine the mRNA expression of NLRP3, total RNA in HIOEC and OSCC cells was extracted using the TRIzol reagent (Invitrogen, San Diego, CA, USA) and real-time PCR were carried out as described previously [23]. The PrimeScript RT Reagent kit (TaKaRa, Shiga, Japan) was adopted for reverse transcription. Real-time PCR was carried out using the SYBR Premix Ex Taq II (TaKaRa) reaction system and cycling conditions were set according to the manufacturer’s instructions.

**Table 1** Correlation between NLRP3 expression and clinicopathological features, IL-1 $\beta$  expression in patients with OSCC ( $n = 77$ )

| Characteristics             | n(77) | NLRP3 expression      |                  |                       | P-value <sup>a</sup> |
|-----------------------------|-------|-----------------------|------------------|-----------------------|----------------------|
|                             |       | negative (20)<br>n(%) | weak(24)<br>n(%) | positive (33)<br>n(%) |                      |
| Age(years)                  |       |                       |                  |                       | 0.436                |
| $\leq 60$                   | 40    | 10 (25)               | 15 (37.5)        | 15 (37.5)             |                      |
| $>60$                       | 37    | 10 (27)               | 9 (24.3)         | 18 (48.7)             |                      |
| Sex                         |       |                       |                  |                       | 0.718                |
| Male                        | 57    | 15 (26.3)             | 19 (33.3)        | 23 (40.4)             |                      |
| Female                      | 20    | 5 (25)                | 5 (25)           | 10 (50)               |                      |
| Smoking status <sup>b</sup> |       |                       |                  |                       | 0.491                |
| Current/former              | 36    | 8 (22.2)              | 10 (27.8)        | 18 (50)               |                      |
| Never                       | 41    | 12 (29.3)             | 14 (34.1)        | 15 (36.6)             |                      |
| Alcohol use <sup>c</sup>    |       |                       |                  |                       | 0.561                |
| Yes                         | 26    | 5 (19.2)              | 8 (30.8)         | 13 (50)               |                      |
| No                          | 51    | 15 (29.4)             | 16 (31.4)        | 20 (39.2)             |                      |
| Location                    |       |                       |                  |                       | 0.403                |
| Gingiva                     | 23    | 4 (17.4)              | 6 (26.1)         | 13 (56.5)             |                      |
| Tongue                      | 31    | 11 (35.5)             | 11 (35.5)        | 9 (29)                |                      |
| Floor of mouth              | 10    | 1 (10)                | 4 (40)           | 5 (50)                |                      |
| Buccal                      | 13    | 4 (30.7)              | 3 (23.1)         | 6 (46.2)              |                      |
| AJCC stage                  |       |                       |                  |                       | 0.018*               |
| I                           | 21    | 10 (47.6)             | 8 (38.1)         | 3(14.3)               |                      |
| II                          | 41    | 8 (19.5)              | 11(26.8)         | 22 (53.7)             |                      |
| III                         | 15    | 2 (13.3)              | 5 (33.3)         | 8 (53.4)              |                      |
| T stage                     |       |                       |                  |                       | 0.015*               |
| T1                          | 9     | 5 (55.6)              | 3 (33.3)         | 1 (11.1)              |                      |
| T2                          | 24    | 10 (43.5)             | 6 (26.1)         | 8(30.4)               |                      |
| T3                          | 28    | 3 (10.7)              | 10(35.7)         | 15 (53.6)             |                      |
| T4                          | 16    | 2 (12.5)              | 5 (31.2)         | 9(56.3)               |                      |
| N stage                     |       |                       |                  |                       | 0.008**              |
| N0                          | 39    | 15(38.5)              | 15 (38.5)        | 9 (23)                |                      |
| N1                          | 23    | 3 (13)                | 6 (26.1)         | 14 (60.9)             |                      |
| N2                          | 15    | 2 (13.3)              | 3 (20)           | 10 (66.7)             |                      |
| IL-1 $\beta$ expression     |       |                       |                  |                       | 0.004**              |
| Negative                    | 21    | 12(57.2)              | 4(19)            | 5(23.8)               |                      |
| Weak                        | 21    | 4(19)                 | 7(33.3)          | 10(47.7)              |                      |
| Positive                    | 35    | 4(11.4)               | 13(37.1)         | 18(51.5)              |                      |

<sup>a</sup>P-values are based on chi-squared or Fisher's exact test.  $P < 0.05$  indicates a significant association among the variables. (\* $P < 0.05$ , \*\* $P < 0.01$ )

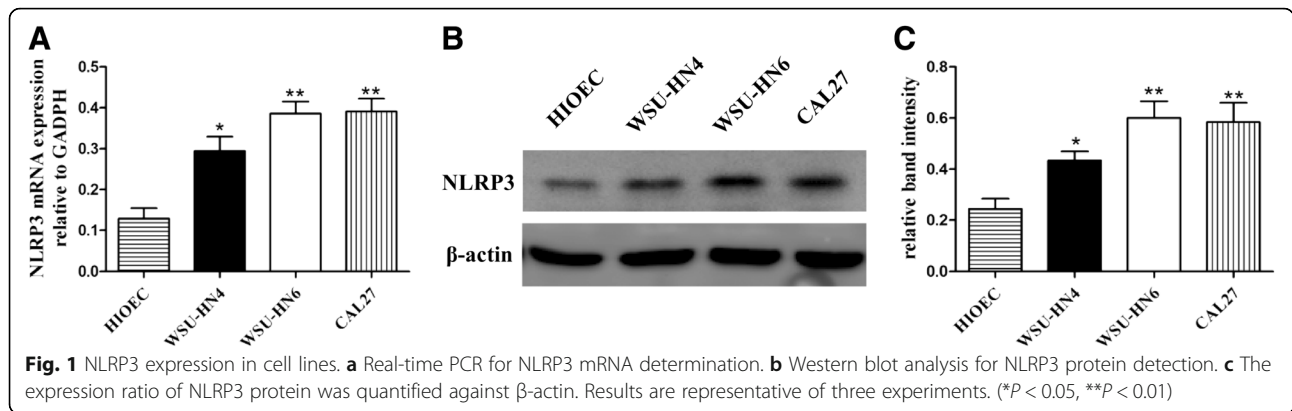
<sup>b</sup>Former/current smokers defined as at least a one pack-year history of smoking

<sup>c</sup>Alcohol intake was defined as current alcohol intake of more than one drink per day for 1 year. Others were classified as no alcohol intake

GAPDH was used as an endogenous control to normalize differences in the amount of total RNA of different samples. Primer sequences were as follows. NLRP3: sense 5'-CCATCGGCAAGACCAAGA-3', anti-sense 5'-ACAGGCTCAGAATGCTCAT C-3'. GAPDH: sense 5'-TGACTTCAACAGCGACACCCA-3', anti-sense 5'-CAC CCTGTTGCTGTAGCCAAA-3'.

#### Western blot analysis

Cells were lysed in Radio Immunoprecipitation Assay (RIPA) buffer (Beyotime Biotechnology, Nanjing, China) and total proteins were denatured after quantification. Same amount of protein was loaded on sodium dodecyl sulfate (SDS) polyacrylamide gels for electrophoresis and then electrophoretically transferred onto polyvinylidene



difluoride (PVDF) membranes (Bio-Rad, Hercules, CA, USA). Non-fat milk powder in Tris-buffered saline (TBS)/Tween20 (TBS/T) with a final concentration of 5% was used to block the non-specific sites. The blots were then incubated with various primary antibodies at 4 °C overnight. Fluorescent-based anti-rabbit or anti-mouse IgG secondary antibody (Fermentas, Vilnius, Lithuania) was used to detect the captured primary antibodies on the membranes. Finally, immunoreactive bands were analyzed by the Odyssey Infrared Imaging System (LI-COR Biosciences, Lincoln, NE, USA).

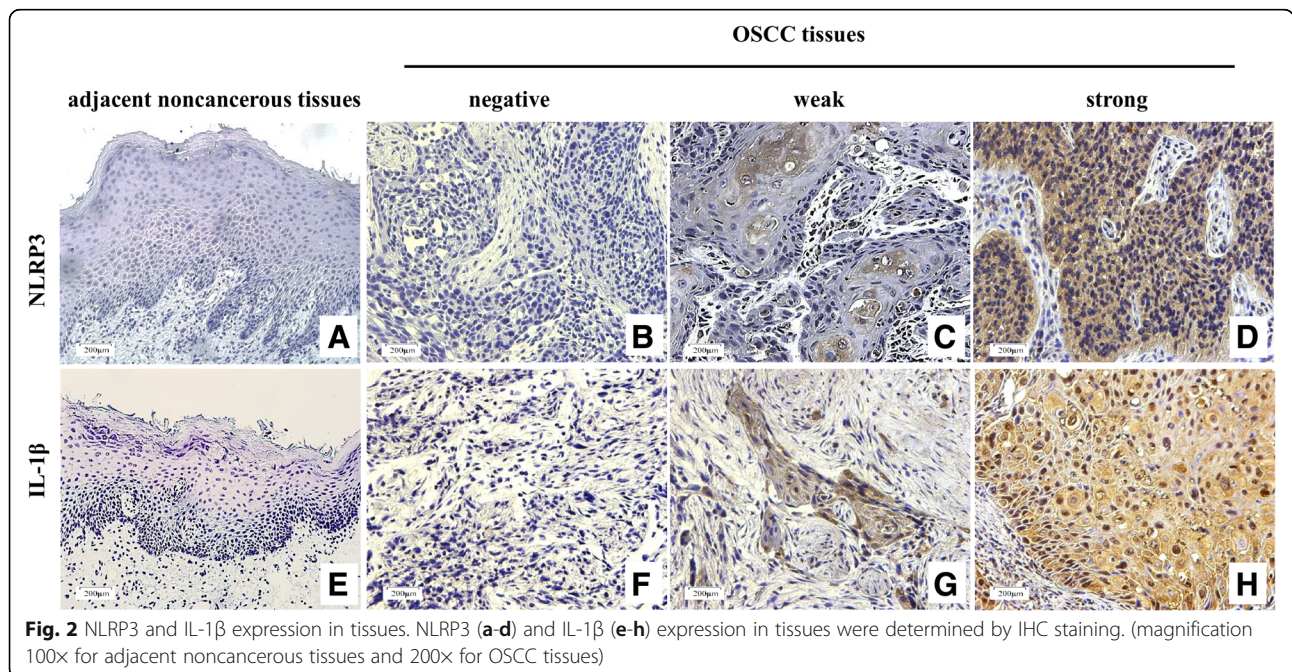
**Gene knockdown**

To knockdown the expression of NLRP3 in OSCC cells, short hairpin RNA (shRNA) were constructed and purchased (Genechem, Shanghai, China) [23]. Sequences of the shRNA duplex targeting NLRP3 (shNLRP3) were: sense 5'-GATCCAGCCAA CAGGAGAAGTTTCCTTCCTGT

CAGAGAAAGTTCTCTCTGTTGGCTTTTTTG-3', anti-sense 5'-AATTCAAAAAAGCCAACAGGAGAAGTTTC TCTGACAGGAAGG AAAGTTCTCTCTGTTGGCTG-3'. The negative control (mock) vector was constructed with a sequence of 5'-GAAGCAGCAGCACTTCTTC-3'. Twelve hours after lentivirus particles transfection, the cells were treated with puromycin for another 7 days to select the stable transfected cells. Real-time PCR and western blot were used to confirm the efficiency of gene knockdown.

**Cell proliferation and colony formation assay**

Cells with different densities were planked into 96-well or 6-well plates and cultured for different time. To determine the cell proliferation, 3-(4,5-dimethylthiazol-2-yl)-2,5-diphenyl tetrazolium bromide (MTT, Sigma) solution was added into each well. After another 4 h incubation, supernatants were discarded and dimethyl sulfoxide (DMSO, Sigma) was supplemented to dissolve the formazan



crystals. Finally, absorbance at wavelength of 490 nm was determined on a microplate reader (Bio-Rad). For colony formation assay, cell clones were stained with a solution containing 0.5% crystal violet and 25% methanol after three weeks' culture. Excess dye was removed by rinses with tap water. Colonies (> 50 cells) were counted under a microscopy.

**Migration and invasion assays**

The migration and invasion assays were performed in 8 μm Transwell Inserts (Corning, New York, USA) for 24 well plates with uncoated membranes or Matrigel (BD Biosciences, San Jose, USA) coated membranes, respectively. Briefly, OSCC cells (2 × 10<sup>4</sup> cells) prepared in DMEM medium were loaded in the upper well, and complete culture medium supplemented with FBS was placed in the lower wells as chemo-attractant. After 12-h or 24-h incubation, the cells that did not penetrate the membrane on the upper chamber were gently removed with a cotton swab. Cells passed through the membrane were fixed and stained with 0.1% crystal violet solution. The inserts were thoroughly rinsed until the water became clear. Finally, cells numbers in the insert were

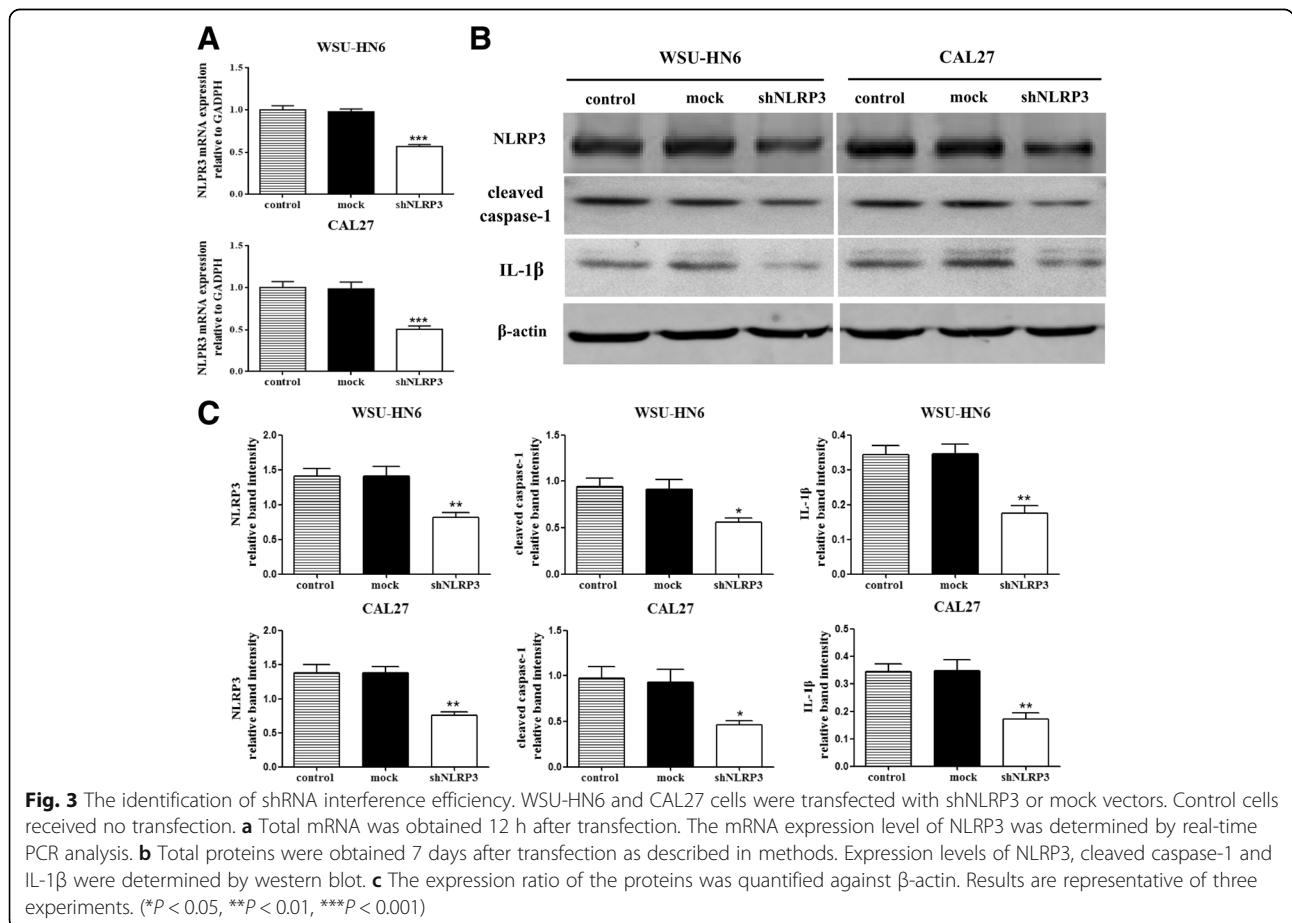
estimated in 6 random fields of views under an inverted microscope.

**Establishment of OSCC xenograft mouse model**

A total of 2 × 10<sup>6</sup> WSU-HN6 cells with or without NLRP3 knockdown were injected subcutaneously into the back next to the right hind limb of the nude mouse and permitted to grow until palpable. Then tumors were measured every 4 days with a vernier caliper and tumor volumes were calculated according to the following formula: tumor volume (mm<sup>3</sup>) = A × B<sup>2</sup> × 0.52. A is the longest diameter and B is the shortest diameter. Tumor-bearing mice were sacrificed at the end of the experiment. After being separated from the surrounding muscles and dermis, tumors were weighed or fixed with 4% phosphate-buffered paraformaldehyde.

**Statistical analysis**

All the presented data and results were confirmed by at least three independent experiments. Data are shown as mean ± SD. The two-tailed Student's *t* test was used to determine the statistical significance of the differences between two groups. The χ<sup>2</sup> test was used to evaluate the relation between NLRP3 expression and different



clinicopathological parameters of the patients, and the Fisher's exact test was used to analyze the relation of NLRP3 expression and IL-1 $\beta$  expression.  $P < 0.05$  was considered statistically significant. All statistical analyses were performed using the SPSS version 19.0 software (SPSS Inc., New York, NY, USA).

## Results

### NLRP3 expression is increased in OSCC cells

To determine the expression levels of NLRP3 in OSCC cells, RT-PCR and western blot analysis were performed. Results indicated that the mRNA expression of NLRP3 was significantly higher in all three OSCC cell lines than that in HIOEC (Fig. 1a). Western blot analysis confirmed the higher expression of NLRP3 in OSCC cells (Fig. 1b and c). Thus, the aberrant overexpression of NLRP3 at the transcriptional and translational levels suggests that NLRP3 may be functionally important in OSCC.

### NLRP3 expression is associated with the clinicopathological characteristics of OSCC patients

To further identify the expression of NLRP3 in tissues, IHC staining was performed in 77 OSCC specimens. The staining score was calculated by multiplying staining proportion score (PS) and staining intensity score (IS). PS was classified as 0 (0%), 1 (1%~25%), 2 (26%~50%), 3 (51%~75%), and 4 (76%~100%). IS was classified as 0

(negative), 1 (weak), 2 (moderate) and 3 (strong). Patients with different expression were divided into three groups: negative expression group (IRS = 0), weak expression group (IRS = 1~3) and strong positive expression group (IRS = 4~12). In the OSCC tissues, positive staining of NLRP3 was observed in 74.03% (57/77) of the cases, with 42.11% (24/57) of weak expression and 57.89% (33/57) of strong expression (Fig. 2b-d and Additional file 1: Table S1). No obvious NLRP3 expression was found in the paired adjacent noncancerous tissues (Fig. 2a). The upregulated expression of NLRP3 was significantly associated with the AJCC stage ( $P = 0.018$ ), T stage ( $P = 0.015$ ) and N stage ( $P = 0.008$ ) of OSCC (Table 1). As the activation of NLRP3 inflammasome leads to the maturation cleavage of pro-IL-1 $\beta$ , we evaluated IL-1 $\beta$  expression simultaneously. Similar expression patterns to NLRP3 were found for IL-1 $\beta$  (Fig. 2e-h), and a positive correlation between the NLRP3 and IL-1 $\beta$  was identified by the Fisher's exact test ( $P = 0.004$ ) (Table 1). Therefore, these data confirm the functional overexpression of NLRP3 in OSCC.

### NLRP3 knockdown inhibits the proliferation of OSCC cells

To clarify the biological significance of NLRP3, NLRP3 short hairpin RNA was constructed and transfected into the OSCC cells. As higher NLRP3 expression was found in WSU-HN6 and CAL27 cells, we chose them for

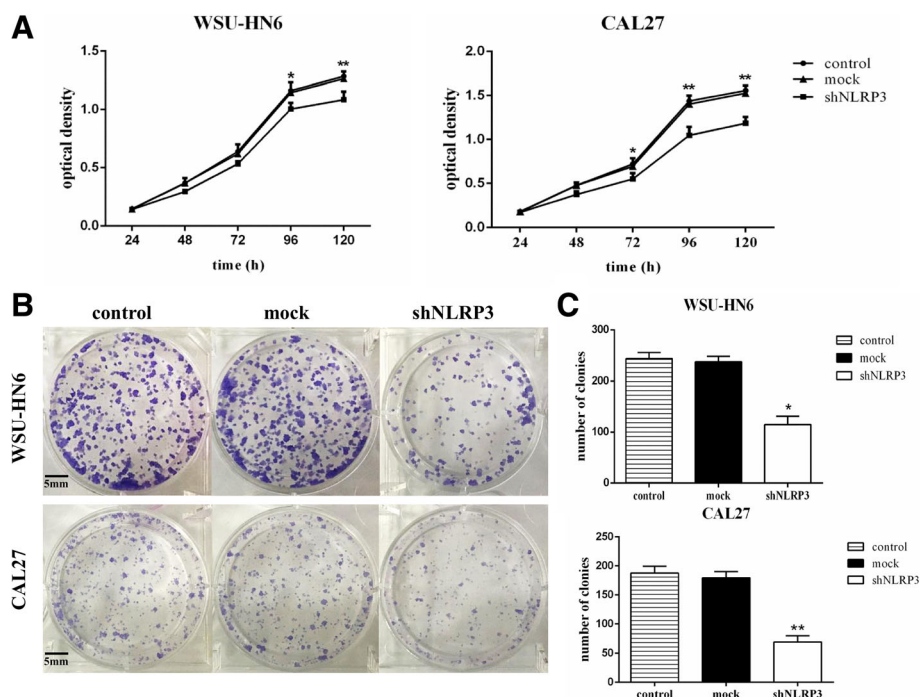


**Fig. 4** NLRP3 knockdown decreases OSCC cell proliferation. WSU-HN6 and CAL27 cells were transfected with shNLRP3 or mock vector. **a** Cell proliferative abilities of the cells were examined by the MTT assay. **b** OSCC cells were seeded into 6-well plates at a density of 800 cells/well. After 2 weeks, the cell clones were stained and photographed. **c** Histograms demonstrated the numbers of colonies in each group. One representative experiment out of three is shown (\* $P < 0.05$ , \*\* $P < 0.01$ )

subsequent studies. The interference efficiency was determined, and markedly reduced NLRP3 expression was observed in OSCC cells after shNLRP3 transfection (Fig. 3). Similar expression patterns were also found for cleaved caspase-1 and IL-1 $\beta$ , which indicated that the function of NLRP3 inflammasome was impaired by NLRP3 knock-down. Then we assessed the proliferative abilities of OSCC cells, and found NLRP3 knockdown significantly decreased the cell viabilities and affected the colony formation of OSCC cells (Fig. 4). Thus, these results suggest that NLRP3 exerts an important role in OSCC cell proliferation.

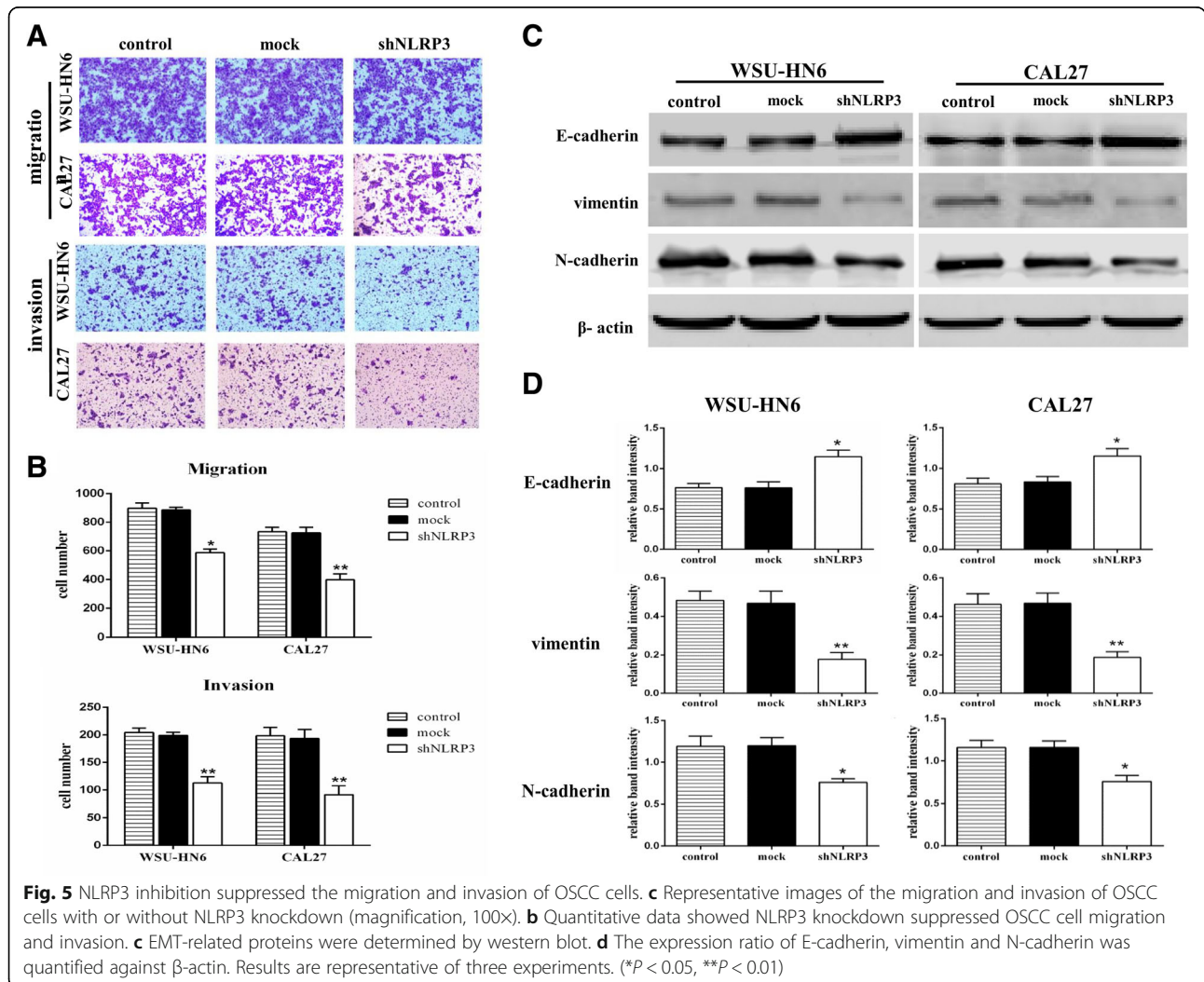
**Decreased NLRP3 expression attenuates OSCC cell migration and invasion**

Since NLRP3 expression was correlated with N stage which indicated the lymphonode metastasis status of OSCC, the effect of NLRP3 knockdown on OSCC cell migration and invasion was examined. Results showed that shNLRP3 transfection significantly decreased the migration and

invasion of OSCC cells (Fig. 5a and b). Considering that the epithelial-mesenchymal transition (EMT) is a critical process in tumor metastasis, in which cancer cells lose epithelial morphology and acquire mesenchymal morphology and invasive phenotype, EMT-related proteins were determined. Consistently, the mesenchymal markers-vimentin and N-cadherin were clearly downregulated, while the epithelial adhesion marker E-cadherin was obviously upregulated in OSCC cells with shNLRP3 transfection (Fig. 5c and d). These data suggest that NLRP3 involves in the metastasis of OSCC cells.

**Suppression of NLRP3 affects OSCC growth in vivo**

To evaluate the effect of NLRP3 knockdown on the growth of OSCC cells in vivo, the OSCC xenograft model was established in nude mice. The parental cells (control), mock vector-transfected cells and shNLRP3-transfected cells (shNLRP3) were subcutaneously implanted into the back of the mice. Tumor volumes were calculated and tumor weights were recorded. Data



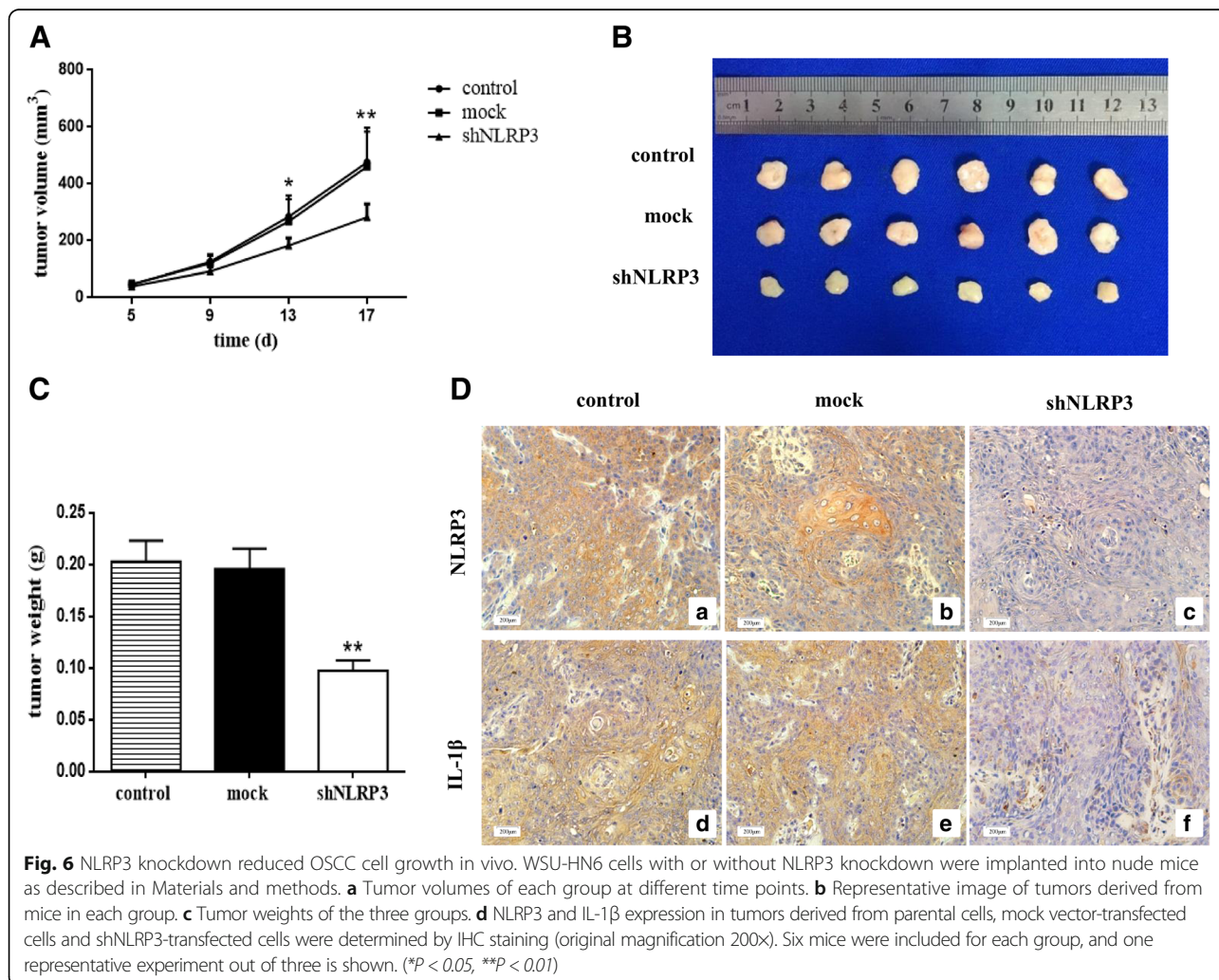
demonstrated that the silencing of NLRP3 distinctly reduced the tumor sizes and weights (Fig. 6a-c). However, the growth of the mock-transfected tumor cells was not affected (Fig. 6a-c). Similar to the in vitro data, decreased expression of NLRP3 and IL-1 $\beta$  was found in tumors derived from shNLRP3-transfected cells compared with those from the control or mock-transfected cells (Fig. 6d). Therefore, NLRP3 silence impaired the function of NLRP3 inflammasome, which led to the suppressed OSCC growth in vivo.

## Discussion

OSCC is the most common head and neck squamous cell carcinoma, which can rise from various locations including the gingiva, tongue, floor of mouth and bucca [24]. The disease develops from precancerous dysplastic lesions through multistep processes of carcinogenesis and the related mechanisms were complex and poorly understood [25, 26]. In our present study, we demonstrated the OSCC-promoting property of NLRP3 both in

vitro and in vivo for the first time. We found that NLRP3 was aberrantly overexpressed in OSCC cells, and the abnormal expression was correlated with the tumor stage, lymph node metastatic status and IL-1 $\beta$  expression level. Knockdown of NLRP3 significantly decreased OSCC cell proliferation, migration and invasion. Moreover, silencing NLRP3 expression significantly inhibited OSCC tumor growth in vivo.

Increasing evidences have emphasized the chronic inflammation is crucial for the initiation, growth and metastasis of cancer [27]. Therefore, the roles of the inflammation related immune molecules have received great attention. The pattern recognition receptors [PRRs, including the Toll-like receptors (TLRs) and NLRs etc.], which recognize the pathogen associated molecular pattern (PAMP) or damage associated molecular pattern (DAMP) and initiate the inflammatory responses, have been observed aberrantly expressed in various cancers [12]. Yang et al. reported that TLR4 was overexpressed in human breast cancer tissue and correlated with lymph





node metastasis [28]. Zhou et al. found high expression of TLR5 correlated with better prognosis in non-small-cell lung cancer [29]. Moreover, TLR7 and TLR9 expression was discovered to be up-regulated in human hepatic cell carcinoma tissue [30]. For NLRs, the intensity of NLRP12 immunostaining was found significantly higher in malignant prostate as compared to their adjacent benign tissues [31]. Paugh et al. found NLRP3 inflammatory upregulation and caspase-1 cleavage of the glucocorticoid receptor caused glucocorticoid resistance in leukemia cells [22]. Our previous studies also reported the abnormal expression of PRRs-TLR3 and TLR4 in OSCC [32, 33]. In this study, we found NLRP3 was overexpressed in OSCC cells, and the expression was associated with the clinicopathological characteristics of the OSCC patients. Thus we inferred that the abnormal expression of NLRP3 in OSCC was functional and went on further investigation.

Previous studies indicated that the effects of NLRP3 inflammasome are complex with differential roles in different types of cancers. In the study of skin cancer, Chow et al. reported that NLRP3 promoted inflammation-induced skin cancer [34]. And in melanoma cells, Okamoto et al. found that overexpressed and constitutively activated NLRP3 inflammasome promoted late stage melanoma progression via the cleaved caspase-1 and active IL-1 $\beta$  [16]. While in colitis-associated cancer, Allen et al. demonstrated that NLRP3 inflammasome in hematopoietic cells, rather than intestinal epithelial cells or stromal cells, functioned as a negative tumorigenesis regulator [35]. Moreover, chemotherapeutic agents may have an effect on the NLRP3 inflammasome of cells existed in the tumor microenvironment. Recently, Bruchard et al. reported that gemcitabine (Gem) and 5-fluorouracil (5-FU) activated the NLRP3 inflammasome in myeloid-derived suppressor cells and led to the secretion of IL-1 $\beta$ , and then the active IL-1 $\beta$  promoted the production of IL-17 by CD4<sup>+</sup> T cells and finally blunted the anticancer efficacy [36]. Thus, in-depth understanding the expression and function of NLRP3 inflammasome may offer new insights into tumor therapy. Our data demonstrated the overexpression of NLRP3 in OSCC cells promoted OSCC tumor growth and metastasis. And 5-FU treatment could further increase the expression and activation of NLRP3 inflammasome in OSCC cells, which in turn attenuated its anti-tumor effect [23]. However, the activation and function of NLRP3 inflammasome in other cells of the OSCC tumor microenvironment needs more exploration.

## Conclusions

In conclusion, our results reveal that the overexpressed NLRP3 contributes to the proliferation and metastasis of OSCC cells. Thus, NLRP3 may be used as a potential target for OSCC treatment.

## Additional file

**Additional file 1: Table S1.** IHC Staining score of the expression levels of NLRP3 and IL-1 $\beta$  in 77 OSCC tissues. The positive grade was determined based on the Immuno-Reactive-Score (IRS), which was calculated by multiplying staining proportion score (PS) and staining intensity score (IS). PS was classified as 0 (0%), 1 (1%–25%), 2 (26%–50%), 3 (51%–75%), and 4 (76%–100%). IS was classified as 0 (negative), 1 (weak), 2 (moderate) and 3 (strong). The final staining score was calculated by multiplying IS by PS. According to the final score, patients with different expression were divided into three groups: negative expression group (IRS = 0), weak expression group (IRS = 1–3) and strong positive expression group (IRS = 4–12). (XLSX 15 kb)

## Abbreviations

5FU: 5-fluorouracil; AJCC: American Joint Committee on Cancer; ASC: Speck-like protein containing CARD; DAMP: Damage associated molecular pattern; DMEM: Dulbecco's modified Eagle medium; DMSO: Dimethyl sulfoxide; EMT: Epithelial-to-mesenchymal transition; FBS: Fetal bovine serum; Gem: Gemcitabine; HIOEC: Human immortalized oral epithelial cells; IHC: Immunohistochemistry; IRS: Immuno-Reactive-Score; IS: Staining intensity score; MTT: 3-(4,5-dimethylthiazol-2-yl)-2,5-diphenyl tetrazolium bromide; NLR: Nucleotide-binding and oligomerization domain (NOD)-like receptor; NLRP3: NLR pyrin domain-containing protein 3; OSCC: Oral squamous cell carcinoma; PAMP: Pathogen associated molecular pattern; PBS: Phosphate-buffered saline; PS: Staining proportion score; PVDF: Polyvinylidene difluoride; RIPA: Radio immunoprecipitation assay; SDS: Sodium dodecyl sulfate

## Acknowledgements

The authors thank the Shanghai Key Laboratory of Stomatology for kindly providing HIOEC and OSCC cell lines.

## Funding

This work was supported by the National Natural Science Foundation of China (81472514 and 81200299) and by the National Program on Key Research Project of China (No.2016YFC0902700, Precision Medicine). The funding bodies had no role in the design of the study and collection, analysis, and interpretation of data and in writing the manuscript.

## Availability of data and materials

The datasets analyzed during the current study are available from the corresponding author on reasonable request.

## Authors' contributions

HW and QQL performed most of the experiments and data analysis, and drafted the manuscript. XDF and RYZ helped to cell culture. JL provided professional advices on the experiment design and reviewed the paper. FXC managed the experimental design, reviewed the manuscript and provided funding support. All authors read and approved the final manuscript.

## Ethics approval

Under the protocol approved by the Review Board of Hospital Ethics Committee, written informed consent was obtained from the patients or their guardians. The Ethical Committee of Shanghai Ninth People's Hospital, Shanghai Jiao Tong University School of Medicine approved the tissue collection and use of the cell lines. All procedures involving animals were performed according to the guidelines of the Association for the Assessment and Accreditation of Laboratory Animal Care International.

## Competing interests

The authors declare that they have no competing interests.

## Publisher's Note

Springer Nature remains neutral with regard to jurisdictional claims in published maps and institutional affiliations.

## Author details

<sup>1</sup>Department of Clinical Immunology, Ninth People's Hospital, Shanghai Jiao Tong University School of Medicine, 639 Zhizaoju Road, Shanghai 200011,

China. <sup>2</sup>Department of Oral Pathology, Ninth People's Hospital, Shanghai Jiao Tong University School of Medicine, Shanghai 200011, China.

Received: 9 August 2017 Accepted: 18 April 2018

Published online: 02 May 2018

## References

- Mignogna MD, Fedele S, Lo RL. The world Cancer report and the burden of oral cancer. *Eur J Cancer Prev.* 2004;13(2):139–42.
- Chi AC, Day TA, Neville BW. Oral cavity and oropharyngeal squamous cell carcinoma—an update. *CA Cancer J Clin.* 2015;65(5):401–21.
- Blatt S, Kruger M, Ziebart T, Sagheb K, Schiegnitz E, Goetze E, Al-Nawas B, Pabst AM. Biomarkers in diagnosis and therapy of oral squamous cell carcinoma: a review of the literature. *J Craniomaxillofac Surg.* 2017;45(5):722–30.
- Warnakulasuriya S. Global epidemiology of oral and oropharyngeal cancer. *Oral Oncol.* 2009;45(4–5):309–16.
- Li N, Grivennikov SI, Karin M. The unholy trinity: inflammation, cytokines, and STAT3 shape the cancer microenvironment. *Cancer Cell.* 2011;19(4):429–31.
- Zitvogel L, Kepp O, Galluzzi L, Kroemer G. Inflammasomes in carcinogenesis and anticancer immune responses. *Nat Immunol.* 2012;13(4):343–51.
- Crusz SM, Balkwill FR. Inflammation and cancer: advances and new agents. *Nat Rev Clin Oncol.* 2015;12(10):584–96.
- Diakos CI, Charles KA, McMillan DC, Clarke SJ. Cancer-related inflammation and treatment effectiveness. *Lancet Oncol.* 2014;15(11):e493–503.
- Mantovani A. Cancer: Inflammation metastasis. *Nature.* 2009;457(7225):36–7.
- de Zoete MR, Palm NW, Zhu S, Flavell RA. Inflammasomes. *Cold Spring Harb Perspect Biol.* 2014;6(12):a016287.
- Schroder K, Tschopp J. The inflammasomes. *Cell.* 2010;140(6):821–32.
- Davis BK, Wen H, Ting JP. The inflammasome NLRs in immunity, inflammation, and associated diseases. *Annu Rev Immunol.* 2011;29:707–35.
- Martinon F, Mayor A, Tschopp J. The inflammasomes: guardians of the body. *Annu Rev Immunol.* 2009;27:229–65.
- Khare S, Luc N, Dorfleutner A, Stehlik C. Inflammasomes and their activation. *Crit Rev Immunol.* 2010;30(5):463–87.
- Takeuchi O, Akira S. Pattern recognition receptors and inflammation. *Cell.* 2010;140(6):805–20.
- Okamoto M, Liu W, Luo Y, Tanaka A, Cai X, Norris DA, Dinarello CA, Fujita M. Constitutively active inflammasome in human melanoma cells mediating autoinflammation via caspase-1 processing and secretion of interleukin-1beta. *J Biol Chem.* 2010;285(9):6477–88.
- Zhai Z, Liu W, Kaur M, Luo Y, Domenico J, Samson JM, et al. NLRP1 promotes tumor growth by enhancing inflammasome activation and suppressing apoptosis in metastatic melanoma. *Oncogene.* 2017;36(27):3820–30.
- Normand S, Delanoye-Crespin A, Bressenot A, Huot L, Grandjean T, Peyrin-Biroulet L, Lemoine Y, Hot D, Chamaillard M. Nod-like receptor pyrin domain-containing protein 6 (NLRP6) controls epithelial self-renewal and colorectal carcinogenesis upon injury. *Proc Natl Acad Sci U S A.* 2011;108(23):9601–6.
- Kolb R, Phan L, Borchering N, Liu Y, Yuan F, Janowski AM, et al. Obesity-associated NLR4 inflammasome activation drives breast cancer progression. *Nat Commun.* 2016;7:13007.
- Poli G, Brancorsini S, Cochetti G, Barillaro F, Egidi MG, Mearini E. Expression of inflammasome-related genes in bladder cancer and their association with cytokeratin 20 messenger RNA. *Urol Oncol.* 2015;33(12):1–7.
- Ng GZ, Menheniott TR, Every AL, Stent A, Judd LM, Chionh YT, et al. The MUC1 mucin protects against helicobacter pylori pathogenesis in mice by regulation of the NLRP3 inflammasome. *Gut.* 2016;65(7):1087–99.
- Paugh SW, Bonten EJ, Savic D, Ramsey LB, Thierfelder WE, Gurung P, et al. NALP3 inflammasome upregulation and CASP1 cleavage of the glucocorticoid receptor cause glucocorticoid resistance in leukemia cells. *Nat Genet.* 2015;47(6):607–14.
- Feng X, Luo Q, Zhang H, Wang H, Chen W, Meng G, Chen F. The role of NLRP3 inflammasome in 5-fluorouracil resistance of oral squamous cell carcinoma. *J Exp Clin Cancer Res.* 2017;36(1):81–94.
- Wang Z, Feng X, Liu X, Jiang L, Zeng X, Ji N, Li J, Li L, Chen Q. Involvement of potential pathways in malignant transformation from oral leukoplakia to oral squamous cell carcinoma revealed by proteomic analysis. *BMC Genomics.* 2009;10:383.
- Brouns E, Baart J, Karagozoglu K, Aartman I, Bloemena E, van der Waal I. Malignant transformation of oral leukoplakia in a well-defined cohort of 144 patients. *Oral Dis.* 2014;20(3):e19–24.
- Lippman SM, Sudbo J, Hong WK. Oral cancer prevention and the evolution of molecular-targeted drug development. *J Clin Oncol.* 2005;23(2):346–56.
- Landskron G, De la Fuente M, Thuwajit P, Thuwajit C, Hermoso MA. Chronic inflammation and cytokines in the tumor microenvironment. *J Immunol Res.* 2014;2014:149185.
- Yang H, Wang B, Wang T, Xu L, He C, Wen H, Yan J, Su H, Zhu X. Toll-like receptor 4 prompts human breast cancer cells invasiveness via lipopolysaccharide stimulation and is overexpressed in patients with lymph node metastasis. *PLoS One.* 2014;9(10):e109980.
- Zhou H, Chen JH, Hu J, Luo YZ, Li F, Xiao L, Zhong MZ. High expression of toll-like receptor 5 correlates with better prognosis in non-small-cell lung cancer: an anti-tumor effect of TLR5 signaling in non-small cell lung cancer. *J Cancer Res Clin Oncol.* 2014;140(4):633–43.
- Mohamed FE, Al-Jehani RM, Minogue SS, Andreola F, Winstanley A, Olde Damink SW, et al. Effect of toll-like receptor 7 and 9 targeted therapy to prevent the development of hepatocellular carcinoma. *Liver Int.* 2015;35(3):1063–76.
- Karan D, Tawfik O, Dubey S. Expression analysis of inflammasome sensors and implication of NLRP12 inflammasome in prostate cancer. *Sci Rep.* 2017;7(1):4378.
- Luo Q, Hu S, Yan M, Sun Z, Chen W, Chen F. Activation of toll-like receptor 3 induces apoptosis of oral squamous carcinoma cells in vitro and in vivo. *Int J Biochem Cell Biol.* 2012;44(8):1266–75.
- Sun Z, Luo Q, Ye D, Chen W, Chen F. Role of toll-like receptor 4 on the immune escape of human oral squamous cell carcinoma and resistance of cisplatin-induced apoptosis. *Mol Cancer.* 2012;11:33–44.
- Chow MT, Tschopp J, Moller A, Smyth MJ. NLRP3 promotes inflammation-induced skin cancer but is dispensable for asbestos-induced mesothelioma. *Immunol Cell Biol.* 2012;90(10):983–6.
- Allen IC, TeKippe EM, Woodford RMT, Uronis JM, Holl EK, Rogers AB, Herfarth HH, Jobin C, Ting JPY. The NLRP3 inflammasome functions as a negative regulator of tumorigenesis during colitis-associated cancer. *J Exp Med.* 2010;207(5):1045–56.
- Bruchard M, Mignot G, Derangere V, Chalmin F, Chevriaux A, Vegran F, et al. Chemotherapy-triggered cathepsin B release in myeloid-derived suppressor cells activates the Nlrp3 inflammasome and promotes tumor growth. *Nat Med.* 2013;19(1):57–64.

Ready to submit your research? Choose BMC and benefit from:

- fast, convenient online submission
- thorough peer review by experienced researchers in your field
- rapid publication on acceptance
- support for research data, including large and complex data types
- gold Open Access which fosters wider collaboration and increased citations
- maximum visibility for your research: over 100M website views per year

At BMC, research is always in progress.

Learn more [biomedcentral.com/submissions](https://www.biomedcentral.com/submissions)

